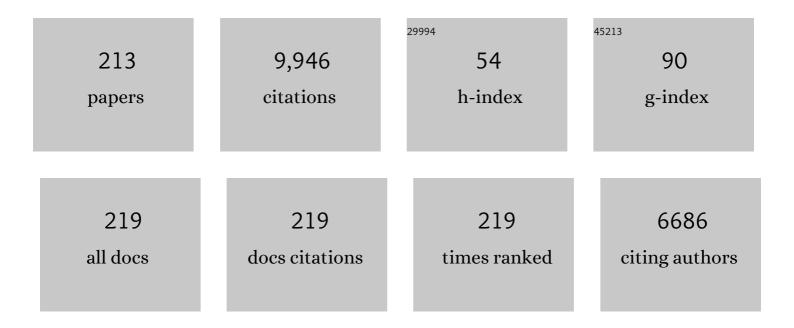
Christoph MÃ¹/₄ller

List of Publications by Year in descending order

Source: https://exaly.com/author-pdf/8251016/publications.pdf Version: 2024-02-01



#	Article	IF	CITATIONS
1	Hydrogen dissociation sites on indium-based ZrO2-supported catalysts for hydrogenation of CO2 to methanol. Catalysis Today, 2022, 387, 38-46.	2.2	11
2	A dilatant, two-layer debris flow model validated by flow density measurements at the Swiss illgraben test site. Landslides, 2022, 19, 265-276.	2.7	7
3	Effect of artificial aggregate shapes on the porosity, tortuosity and permeability of their packings. Powder Technology, 2022, 397, 117019.	2.1	9
4	Sinking dynamics and splitting of a granular droplet. Physical Review Fluids, 2022, 7, .	1.0	2
5	Surface Intermediates in In-Based ZrO ₂ -Supported Catalysts for Hydrogenation of CO ₂ to Methanol. Journal of Physical Chemistry C, 2022, 126, 1793-1799.	1.5	10
6	CO2 hydrogenation to methanol on tungsten-doped Cu/CeO2 catalysts. Applied Catalysis B: Environmental, 2022, 306, 121098.	10.8	50
7	Amyloid fibril-UiO-66-NH ₂ aerogels for environmental remediation. Chemical Communications, 2022, 58, 5104-5107.	2.2	7
8	Bulk and surface transformations of Ga2O3 nanoparticle catalysts for propane dehydrogenation induced by a H2 treatment. Journal of Catalysis, 2022, 408, 155-164.	3.1	18
9	Na-β-Al ₂ O ₃ stabilized Fe ₂ O ₃ oxygen carriers for chemical looping water splitting: correlating structure with redox stability. Journal of Materials Chemistry A, 2022, 10, 10692-10700.	5.2	10
10	Atomic-scale changes of silica-supported catalysts with nanocrystalline or amorphous gallia phases: implications of hydrogen pretreatment on their selectivity for propane dehydrogenation. Catalysis Science and Technology, 2022, 12, 3957-3968.	2.1	7
11	Highly Selective Oxidative Dehydrogenation of Ethane to Ethylene via Chemical Looping with Oxygen Uncoupling through Structural Engineering of the Oxygen Carrier. Advanced Energy Materials, 2022, 12, .	10.2	18
12	Prospects of MgO-based sorbents for CO2 capture applications at high temperatures. Current Opinion in Green and Sustainable Chemistry, 2022, 36, 100645.	3.2	8
13	Model structures of molten salt-promoted MgO to probe the mechanism of MgCO ₃ formation during CO ₂ capture at a solid–liquid interface. Journal of Materials Chemistry A, 2022, 10, 16803-16812.	5.2	9
14	Chemical Looping Partial Oxidation of Methane: Reducing Carbon Deposition through Alloying. Energy & Fuels, 2022, 36, 9780-9784.	2.5	7
15	Metal-oxide stabilized CaO/CuO composites for the integrated Ca/Cu looping process. Chemical Engineering Journal, 2021, 403, 126330.	6.6	28
16	Solar-driven valorisation of glycerol on BiVO ₄ photoanodes: effect of co-catalyst and reaction media on reaction selectivity. Journal of Materials Chemistry A, 2021, 9, 6252-6260.	5.2	34
17	Propane Dehydrogenation on Ga ₂ O ₃ -Based Catalysts: Contrasting Performance with Coordination Environment and Acidity of Surface Sites. ACS Catalysis, 2021, 11, 907-924.	5.5	55
18	Combined Syngas and Hydrogen Production using Gas Switching Technology. Industrial & Engineering Chemistry Research, 2021, 60, 3516-3531.	1.8	13

#	Article	IF	CITATIONS
19	Phase transitions in germanium telluride nanoparticle phase-change materials studied by temperature-resolved x-ray diffraction. Journal of Applied Physics, 2021, 129, 095102.	1.1	2
20	Single-Atom-Substituted Mo ₂ C <i>T</i> _{<i>x</i>} :Fe-Layered Carbide for Selective Oxygen Reduction to Hydrogen Peroxide: Tracking the Evolution of the MXene Phase. Journal of the American Chemical Society, 2021, 143, 5771-5778.	6.6	61
21	Atomic-Scale Structure and Its Impact on Chemical Properties of Aluminum Oxide Layers Prepared by Atomic Layer Deposition on Silica. Chemistry of Materials, 2021, 33, 3335-3348.	3.2	23
22	Reduction in minimum fluidization velocity and minimum bubbling velocity in gas-solid fluidized beds due to vibration. Powder Technology, 2021, 382, 566-572.	2.1	11
23	Preventing Agglomeration of CuO-Based Oxygen Carriers for Chemical Looping Applications. ACS Sustainable Chemistry and Engineering, 2021, 9, 5972-5980.	3.2	36
24	Assessment of the Effect of Process Conditions and Material Characteristics of Alkali Metal Salt Promoted MgO-Based Sorbents on Their CO ₂ Capture Performance. ACS Sustainable Chemistry and Engineering, 2021, 9, 6659-6672.	3.2	32
25	Peering into buried interfaces with X-rays and electrons to unveil MgCO ₃ formation during CO ₂ capture in molten salt-promoted MgO. Proceedings of the National Academy of Sciences of the United States of America, 2021, 118, .	3.3	26
26	Accurate buoyancy and drag force models to predict particle segregation in vibrofluidized beds. Physical Review E, 2021, 103, 062903.	0.8	7
27	Transformation of TiO2 (nano)particles during sewage sludge incineration. Journal of Hazardous Materials, 2021, 411, 124932.	6.5	5
28	Mechanism of anomalous sinking of an intruder in a granular packing close to incipient fluidization. Physical Review Fluids, 2021, 6, .	1.0	7
29	Correlating the Structural Evolution of ZnO/Al ₂ O ₃ to Spinel Zinc Aluminate with its Catalytic Performance in Propane Dehydrogenation. Journal of Physical Chemistry C, 2021, 125, 14065-14074.	1.5	14
30	Ruthenium-Exsolution Catalyst for Dry Reforming of Biogas. ECS Transactions, 2021, 103, 1563-1578.	0.3	1
31	CO ₂ Capture at Medium to High Temperature Using Solid Oxide-Based Sorbents: Fundamental Aspects, Mechanistic Insights, and Recent Advances. Chemical Reviews, 2021, 121, 12681-12745.	23.0	177
32	Photo-Switchable Nanoripples in Ti ₃ C ₂ <i>T</i> _{<i>x</i>} MXene. ACS Nano, 2021, 15, 14071-14079.	7.3	11
33	Two-dimensional molybdenum carbide 2D-Mo2C as a superior catalyst for CO2 hydrogenation. Nature Communications, 2021, 12, 5510.	5.8	63
34	Experimental data supported techno-economic assessment of the oxidative dehydrogenation of ethane through chemical looping with oxygen uncoupling. Renewable and Sustainable Energy Reviews, 2021, 149, 111403.	8.2	13
35	Release of gold (Au), silver (Ag) and cerium dioxide (CeO2) nanoparticles from sewage sludge incineration ash. Environmental Science: Nano, 2021, 8, 3220-3232.	2.2	4
36	Structural insight into an atomic layer deposition (ALD) grown Al ₂ O ₃ layer on Ni/SiO ₂ : impact on catalytic activity and stability in dry reforming of methane. Catalysis Science and Technology, 2021, 11, 7563-7577.	2.1	10

Christoph MÃ¹/4ller

#	Article	IF	CITATIONS
37	Engineering the Cu/Mo2CTx (MXene) interface to drive CO2 hydrogenation to methanol. Nature Catalysis, 2021, 4, 860-871.	16.1	138
38	Uncovering selective and active Ga surface sites in gallia–alumina mixed-oxide propane dehydrogenation catalysts by dynamic nuclear polarization surface enhanced NMR spectroscopy. Chemical Science, 2021, 12, 15273-15283.	3.7	10
39	Lift force acting on an intruder in dense, granular shear flows. Physical Review E, 2021, 104, 064903.	0.8	1
40	Combined Partial Oxidation of Methane to Synthesis Gas and Production of Hydrogen or Carbon Monoxide in a Fluidized Bed using Lattice Oxygen. Energy Technology, 2020, 8, 1900655.	1.8	13
41	Regimes of jetting and bubbling in a fluidized bed studied using real-time magnetic resonance imaging. Chemical Engineering Journal, 2020, 383, 123185.	6.6	24
42	Spatially resolved NMR spectroscopy of heterogeneous gas phase hydrogenation of 1,3-butadiene with <i>para</i> hydrogen. Catalysis Science and Technology, 2020, 10, 99-104.	2.1	16
43	Development of an effective bi-functional Ni–CaO catalyst-sorbent for the sorption-enhanced water gas shift reaction through structural optimization and the controlled deposition of a stabilizer by atomic layer deposition. Sustainable Energy and Fuels, 2020, 4, 713-729.	2.5	20
44	CaO-Based CO ₂ Sorbents with a Hierarchical Porous Structure Made via Microfluidic Droplet Templating. Industrial & Engineering Chemistry Research, 2020, 59, 7182-7188.	1.8	29
45	Exsolution of Metallic Ru Nanoparticles from Defective, Fluorite-Type Solid Solutions Sm ₂ Ru <i>_x</i> Ce _{2–<i>x</i>} O ₇ To Impart Stability on Dry Reforming Catalysts. ACS Catalysis, 2020, 10, 1923-1937.	5.5	70
46	A Dirichlet boundary condition for the thermal lattice Boltzmann method. International Journal of Multiphase Flow, 2020, 123, 103184.	1.6	21
47	Mechanistic Understanding of CaOâ€Based Sorbents for Highâ€Temperature CO ₂ Capture: Advanced Characterization and Prospects. ChemSusChem, 2020, 13, 6259-6272.	3.6	38
48	CO2-free conversion of CH4 to syngas using chemical looping. Applied Catalysis B: Environmental, 2020, 278, 119328.	10.8	48
49	Deciphering the Nature of Ru Sites in Reductively Exsolved Oxides with Electronic and Geometric Metal–Support Interactions. Journal of Physical Chemistry C, 2020, 124, 25299-25307.	1.5	18
50	<i>Operando</i> X-ray Absorption Spectroscopy Identifies a Monoclinic ZrO ₂ :In Solid Solution as the Active Phase for the Hydrogenation of CO ₂ to Methanol. ACS Catalysis, 2020, 10, 10060-10067.	5.5	54
51	Manufacturing complex Al ₂ O ₃ ceramic structures using consumer-grade fused deposition modelling printers. Rapid Prototyping Journal, 2020, 26, 1035-1048.	1.6	29
52	Modern X-ray spectroscopy: XAS and XES in the laboratory. Coordination Chemistry Reviews, 2020, 423, 213466.	9.5	112
53	Atomic-Scale Insight into the Structure of Metastable γ-Ga ₂ O ₃ Nanocrystals and their Thermally-Driven Transformation to β-Ga ₂ O ₃ . Journal of Physical Chemistry C, 2020, 124, 20578-20588.	1.5	24
54	Oxidative dehydrogenation of propane on silica-supported vanadyl sites promoted with sodium metavanadate. Catalysis Science and Technology, 2020, 10, 7186-7193.	2.1	2

#	Article	IF	CITATIONS
55	Na ₂ CO ₃ -modified CaO-based CO ₂ sorbents: the effects of structure and morphology on CO ₂ uptake. Physical Chemistry Chemical Physics, 2020, 22, 24697-24703.	1.3	22
56	Particle-shape induced radial segregation in rotating cylinders. Granular Matter, 2020, 22, 1.	1.1	19
57	Hydrogen production by water splitting using gas switching technology. Powder Technology, 2020, 370, 48-63.	2.1	5
58	Molybdenum carbide and oxycarbide from carbon-supported MoO ₃ nanosheets: phase evolution and DRM catalytic activity assessed by TEM and <i>in situ</i> XANES/XRD methods. Nanoscale, 2020, 12, 13086-13094.	2.8	21
59	Effect of molten sodium nitrate on the decomposition pathways of hydrated magnesium hydroxycarbonate to magnesium oxide probed by <i>in situ</i> total scattering. Nanoscale, 2020, 12, 16462-16473.	2.8	16
60	Tailoring Lattice Oxygen Binding in Ruthenium Pyrochlores to Enhance Oxygen Evolution Activity. Journal of the American Chemical Society, 2020, 142, 7883-7888.	6.6	210
61	Chemical looping beyond combustion – a perspective. Energy and Environmental Science, 2020, 13, 772-804.	15.6	325
62	Gas-solid heat transfer in assemblies of cubes for ReÂâ‰Â100. Chemical Engineering Science, 2020, 216, 115478.	1.9	10
63	Reducibility and Dispersion Influence the Activity in Silica-Supported Vanadium-Based Catalysts for the Oxidative Dehydrogenation of Propane: The Case of Sodium Decavanadate. ACS Catalysis, 2020, 10, 2314-2321.	5.5	22
64	Synchrotron hard X-ray chemical imaging of trace element speciation in heterogeneous samples: development of criteria for uncertainty analysis. Journal of Analytical Atomic Spectrometry, 2020, 35, 567-579.	1.6	6
65	Structural and thermodynamic study of Ca A- or Co B-site substituted SrFeO _{3â^î} perovskites for low temperature chemical looping applications. Physical Chemistry Chemical Physics, 2020, 22, 9272-9282.	1.3	34
66	Exploiting two-dimensional morphology of molybdenum oxycarbide to enable efficient catalytic dry reforming of methane. Nature Communications, 2020, 11, 4920.	5.8	78
67	Asynchronous bubble pinch-off pattern arising in fluidized beds due to jet interaction: A magnetic resonance imaging and computational modeling study. Physical Review Fluids, 2020, 5, .	1.0	6
68	Link between packing morphology and the distribution of contact forces and stresses in packings of highly nonconvex particles. Physical Review E, 2020, 102, 062902.	0.8	9
69	Robust In Situ Magnetic Resonance Imaging of Heterogeneous Catalytic Hydrogenation with and without Hyperpolarization. ChemCatChem, 2019, 11, 969-973.	1.8	7
70	Structural Evolution and Dynamics of an In ₂ O ₃ Catalyst for CO ₂ Hydrogenation to Methanol: An Operando XAS-XRD and In Situ TEM Study. Journal of the American Chemical Society, 2019, 141, 13497-13505.	6.6	204
71	Bifunctional core-shell architecture allows stable H2 production utilizing CH4 and CO2 in a catalytic chemical looping process. Applied Catalysis B: Environmental, 2019, 258, 117946.	10.8	34
72	Transformation of Nanoscale and Ionic Cu and Zn during the Incineration of Digested Sewage Sludge (Biosolids). Environmental Science & Technology, 2019, 53, 11704-11713.	4.6	19

#	Article	IF	CITATIONS
73	Inverse Opal-Like, Ca ₃ Al ₂ O ₆ -Stabilized, CaO-Based CO ₂ Sorbent: Stabilization of a Highly Porous Structure To Improve Its Cyclic CO ₂ Uptake. ACS Applied Energy Materials, 2019, 2, 6461-6471.	2.5	26
74	Magnetic resonance imaging of interaction and coalescence of two bubbles injected consecutively into an incipiently fluidized bed. Chemical Engineering Science, 2019, 208, 115152.	1.9	11
75	Single Site Cobalt Substitution in 2D Molybdenum Carbide (MXene) Enhances Catalytic Activity in the Hydrogen Evolution Reaction. Journal of the American Chemical Society, 2019, 141, 17809-17816.	6.6	259
76	Bi-functional Ru/Ca3Al2O6–CaO catalyst-CO2 sorbent for the production of high purity hydrogen via sorption-enhanced steam methane reforming. Catalysis Science and Technology, 2019, 9, 5745-5756.	2.1	25
77	Real-time magnetic resonance imaging of fluidized beds with internals. Chemical Engineering Science, 2019, 198, 117-123.	1.9	22
78	CO ₂ Uptake and Cyclic Stability of MgO-Based CO ₂ Sorbents Promoted with Alkali Metal Nitrates and Their Eutectic Mixtures. ACS Applied Energy Materials, 2019, 2, 1295-1307.	2.5	79
79	In Situ XANES/XRD Study of the Structural Stability of Two-Dimensional Molybdenum Carbide Mo ₂ CT <i>_x</i> : Implications for the Catalytic Activity in the Water–Gas Shift Reaction. Chemistry of Materials, 2019, 31, 4505-4513.	3.2	100
80	Gravitational instabilities in binary granular materials. Proceedings of the National Academy of Sciences of the United States of America, 2019, 116, 9263-9268.	3.3	24
81	Reversible Exsolution of Dopant Improves the Performance of Ca ₂ Fe ₂ O ₅ for Chemical Looping Hydrogen Production. ACS Applied Materials & Interfaces, 2019, 11, 18276-18284.	4.0	50
82	Magnetic resonance imaging of single bubbles injected into incipiently fluidized beds. Chemical Engineering Science, 2019, 200, 147-166.	1.9	27
83	Wake volume of injected bubbles in fluidized beds: A magnetic resonance imaging velocimetry study. Powder Technology, 2019, 357, 428-435.	2.1	11
84	Characteristics of a single jet injected into an incipiently fluidized bed: A magnetic resonance imaging study. Advanced Powder Technology, 2019, 30, 3146-3152.	2.0	4
85	Transformations of FCC catalysts and carbonaceous deposits during repeated reaction-regeneration cycles. Catalysis Science and Technology, 2019, 9, 6977-6992.	2.1	17
86	Lattice Boltzmann simulation of gas-solid heat transfer in random assemblies of spheres: The effect of solids volume fraction on the average Nusselt number for Reâ€â‰≇€100. Chemical Engineering Journal, 2019, 361, 1392-1399.	6.6	24
87	Oxidation of ammonia by iron, manganese and nickel oxides – Implications on NOx formation in chemical-looping combustion. Fuel, 2019, 240, 57-63.	3.4	23
88	Effect of liquid bridging on bubbles injected into a fluidized bed: A magnetic resonance imaging study. Powder Technology, 2019, 343, 813-820.	2.1	21
89	Anomalous collapse of interacting bubbles in a fluidized bed: A magnetic resonance imaging study. Physical Review Fluids, 2019, 4, .	1.0	11
90	Redox-Driven Restructuring of FeMnZr-Oxygen Carriers Enhances the Purity and Yield of H ₂ in a Chemical Looping Process. ACS Applied Energy Materials, 2018, 1, 1294-1303.	2.5	14

#	Article	IF	CITATIONS
91	The effect of copper on the redox behaviour of iron oxide for chemical-looping hydrogen production probed by <i>in situ</i> X-ray absorption spectroscopy. Physical Chemistry Chemical Physics, 2018, 20, 12736-12745.	1.3	18
92	Integrated CO ₂ Capture and Conversion as an Efficient Process for Fuels from Greenhouse Gases. ACS Catalysis, 2018, 8, 2815-2823.	5.5	168
93	<i>In Situ</i> XRD and Dynamic Nuclear Polarization Surface Enhanced NMR Spectroscopy Unravel the Deactivation Mechanism of CaO-Based, Ca ₃ Al ₂ O ₆ -Stabilized CO ₂ Sorbents. Chemistry of Materials, 2018, 30, 1344-1352.	3.2	40
94	CO ₂ Uptake Potential of Ca-Based Air Pollution Control Residues over Repeated Carbonation–Calcination Cycles. Energy & Fuels, 2018, 32, 5386-5395.	2.5	20
95	Magnetic resonance imaging of gas–solid fluidization with liquid bridging. AICHE Journal, 2018, 64, 2958-2971.	1.8	25
96	A critical assessment of the testing conditions of CaO-based CO2 sorbents. Chemical Engineering Journal, 2018, 336, 544-549.	6.6	47
97	Atomic Layer Deposition of a Film of Al ₂ O ₃ on Electrodeposited Copper Foams To Yield Highly Effective Oxygen Carriers for Chemical Looping Combustion-Based CO ₂ Capture. ACS Applied Materials & Interfaces, 2018, 10, 37994-38005.	4.0	7
98	Self-activated, nanostructured composite for improved CaL-CLC technology. Chemical Engineering Journal, 2018, 351, 1038-1046.	6.6	63
99	Real-Time Magnetic Resonance Imaging of Bubble Behavior and Particle Velocity in Fluidized Beds. Industrial & Engineering Chemistry Research, 2018, 57, 9674-9682.	1.8	36
100	Optimization of the structural characteristics of CaO and its effective stabilization yield high-capacity CO2 sorbents. Nature Communications, 2018, 9, 2408.	5.8	167
101	Combustion of Sewage Sludge: Kinetics and Speciation of the Combustible. Energy & Fuels, 2018, 32, 10656-10667.	2.5	10
102	Development of a drag force correlation for assemblies of cubic particles: The effect of solid volume fraction and Reynolds number. Chemical Engineering Science, 2018, 192, 1157-1166.	1.9	28
103	Segregation of equal-sized particles of different densities in a vertically vibrated fluidized bed. Powder Technology, 2017, 316, 101-110.	2.1	28
104	Cooperativity and Dynamics Increase the Performance of NiFe Dry Reforming Catalysts. Journal of the American Chemical Society, 2017, 139, 1937-1949.	6.6	322
105	Reversal of gulf stream circulation in a vertically vibrated triangular fluidized bed. Powder Technology, 2017, 316, 345-356.	2.1	2
106	Molecularly Tailored Nickel Precursor and Support Yield a Stable Methane Dry Reforming Catalyst with Superior Metal Utilization. Journal of the American Chemical Society, 2017, 139, 6919-6927.	6.6	111
107	The parameters governing the coefficient of dispersion of cubes in rotating cylinders. Granular Matter, 2017, 19, 1.	1.1	14
108	Formation of NiO nanoparticle-attached nanographitic flake layersÂdeposited by pulsed electrophoretic deposition for ethanol electro-oxidation. Journal of Alloys and Compounds, 2017, 698, 571-576.	2.8	14

Christoph Müller

#	Article	IF	CITATIONS
109	Contrasting the Role of Ni/Al ₂ O ₃ Interfaces in Water–Gas Shift and Dry Reforming of Methane. Journal of the American Chemical Society, 2017, 139, 17128-17139.	6.6	172
110	Development of High-performance CaO-based CO2 Sorbents Stabilized with Al2O3 or MgO. Energy Procedia, 2017, 114, 158-166.	1.8	22
111	CaOâ€Based CO ₂ Sorbents Effectively Stabilized by Metal Oxides. ChemPhysChem, 2017, 18, 3280-3285.	1.0	27
112	Multishelled CaO Microspheres Stabilized by Atomic Layer Deposition of Al ₂ O ₃ for Enhanced CO ₂ Capture Performance. Advanced Materials, 2017, 29, 1702896.	11.1	126
113	Supported Bimetallic NiFe Nanoparticles through Colloid Synthesis for Improved Dry Reforming Performance. ACS Catalysis, 2017, 7, 6942-6948.	5.5	77
114	Real-time probing of granular dynamics with magnetic resonance. Science Advances, 2017, 3, e1701879.	4.7	50
115	Development of Fe2O3-based, Al2O3-stabilized Oxygen Carriers using Sol-gel Technique for H2 Production via Chemical Looping. Energy Procedia, 2017, 114, 436-445.	1.8	20
116	Sol-gel Synthesis of MgAl2O4-stabilized CaO for CO2 Capture. Energy Procedia, 2017, 114, 220-229.	1.8	17
117	Platform Chemicals via Zeolite atalyzed Fast Pyrolysis of Glucose. ChemCatChem, 2017, 9, 1579-1582.	1.8	12
118	Chemical Looping for Energy Technology: A Special Issue. Energy Technology, 2016, 4, 1127-1129.	1.8	5
119	Axial dispersion of granular material in inclined rotating cylinders with bulk flow: Geometric model for 50% fill. Powder Technology, 2016, 290, 91-96.	2.1	2
120	Dry-reforming of methane over bimetallic Ni–M/La2O3 (M = Co, Fe): The effect of the rate of La2O2CO3 formation and phase stability on the catalytic activity and stability. Journal of Catalysis, 2016, 343, 208-214.	3.1	131
121	Ordering and stress transmission in packings of straight and curved spherocylinders. Granular Matter, 2016, 18, 1.	1.1	4
122	Modelling – from molecules to mega-scale: general discussion. Faraday Discussions, 2016, 192, 493-509.	1.6	0
123	ZrO ₂ -Supported Fe ₂ O ₃ for Chemical-Looping-Based Hydrogen Production: Effect of pH on Its Structure and Performance As Probed by X-ray Absorption Spectroscopy and Electrical Conductivity Measurements. Journal of Physical Chemistry C, 2016, 120, 18977-18985.	1.5	21
124	Mechanochemically Activated, Calcium Oxideâ€Based, Magnesium Oxideâ€Stabilized Carbon Dioxide Sorbents. ChemSusChem, 2016, 9, 2380-2390.	3.6	40
125	CCS – A technology for now: general discussion. Faraday Discussions, 2016, 192, 125-151.	1.6	5
126	End use and disposal of CO ₂ – storage or utilisation?: general discussion. Faraday Discussions, 2016, 192, 561-579.	1.6	10

Christoph Müller

#	Article	IF	CITATIONS
127	The development of effective CaO-based CO ₂ sorbents via a sacrificial templating technique. Faraday Discussions, 2016, 192, 85-95.	1.6	26
128	Na ⁺ doping induced changes in the reduction and charge transport characteristics of Al ₂ O ₃ -stabilized, CuO-based materials for CO ₂ capture. Physical Chemistry Chemical Physics, 2016, 18, 12278-12288.	1.3	16
129	Comparison between finite volume and lattice-Boltzmann method simulations of gas-fluidised beds: bed expansion and particle–fluid interaction force. Computational Particle Mechanics, 2016, 3, 373-381.	1.5	24
130	Single-Step Electrophoretic Deposition of Non-noble Metal Catalyst Layer with Low Onset Voltage for Ethanol Electro-oxidation. ACS Applied Materials & Interfaces, 2016, 8, 15975-15984.	4.0	29
131	Transformation of Silver Nanoparticles in Sewage Sludge during Incineration. Environmental Science & Technology, 2016, 50, 3503-3510.	4.6	66
132	Development of MgAl ₂ O ₄ -stabilized, Cu-doped, Fe ₂ O ₃ -based oxygen carriers for thermochemical water-splitting. Journal of Materials Chemistry A, 2016, 4, 113-123.	5.2	57
133	Highly Efficient Oxygenâ€Storage Material with Intrinsic Coke Resistance for Chemical Looping Combustionâ€Based CO ₂ Capture. ChemSusChem, 2015, 8, 2055-2065.	3.6	25
134	Development of a Steel‣lagâ€Based, Ironâ€Functionalized Sorbent for an Autothermal Carbon Dioxide Capture Process. ChemSusChem, 2015, 8, 3839-3846.	3.6	30
135	Synthetic calcium oxide-based carbon dioxide sorbents forÂcalcium looping processes. , 2015, , 51-72.		2
136	Ca–Cu looping process for CO2 capture from a power plant and its comparison with Ca-looping, oxy-combustion and amine-based CO2 capture processes. International Journal of Greenhouse Gas Control, 2015, 43, 198-212.	2.3	40
137	Experimental investigation of axial dispersion in a horizontal rotating cylinder. Granular Matter, 2015, 17, 43-48.	1.1	9
138	Ethanol electro-oxidation on nanoworm-shaped Pd particles supported by nanographitic layers fabricated by electrophoretic deposition. RSC Advances, 2015, 5, 52578-52587.	1.7	20
139	Modelling axial dispersion of granular material in inclined rotating cylinders with bulk flow. Granular Matter, 2015, 17, 33-41.	1.1	10
140	CuO promoted Mn ₂ O ₃ -based materials for solid fuel combustion with inherent CO ₂ capture. Journal of Materials Chemistry A, 2015, 3, 10545-10550.	5.2	33
141	Discrete element models for non-spherical particle systems: From theoretical developments to applications. Chemical Engineering Science, 2015, 127, 425-465.	1.9	434
142	A drag force correlation for approximately cubic particles constructed from identical spheres. Chemical Engineering Science, 2015, 123, 146-154.	1.9	26
143	Life Cycle Assessment of Natural Gas-based Chemical Looping for Hydrogen Production. Energy Procedia, 2014, 63, 7408-7420.	1.8	23
144	Development of Highly Effective CaOâ€based, MgOâ€stabilized CO ₂ Sorbents via a Scalable "Oneâ€Pot―Recrystallization Technique. Advanced Functional Materials, 2014, 24, 5753-5761.	7.8	66

#	Article	IF	CITATIONS
145	Effect of wall rougheners on cross-sectional flow characteristics for non-spherical particles in a horizontal rotating cylinder. Particuology, 2014, 12, 44-53.	2.0	25
146	Magnetic resonance imaging (MRI) of jet height hysteresis in packed beds. Chemical Engineering Science, 2014, 109, 276-283.	1.9	15
147	Effect of particle shape on domino wave propagation: a perspective from 3D, anisotropic discrete element simulations. Granular Matter, 2014, 16, 107-114.	1.1	14
148	Effect of Pelletization and Addition of Steam on the Cyclic Performance of Carbon-Templated, CaO-Based CO ₂ Sorbents. Environmental Science & Technology, 2014, 48, 5322-5328.	4.6	78
149	Sol–gel-derived, CaO-based, ZrO2-stabilized CO2 sorbents. Fuel, 2014, 127, 94-100.	3.4	159
150	Structure–property relationship of co-precipitated Cu-rich, Al2O3- or MgAl2O4-stabilized oxygen carriers for chemical looping with oxygen uncoupling (CLOU). Applied Energy, 2014, 119, 557-565.	5.1	60
151	CO2 Capture via Cyclic Calcination and Carbonation Reactions. Green Chemistry and Sustainable Technology, 2014, , 181-222.	0.4	5
152	Magnetic resonance imaging (MRI) study of jet formation in packed beds. Chemical Engineering Science, 2013, 97, 406-412.	1.9	18
153	Statistical accuracy of scattered points filters and application to the dynamics of bubbles in gas-fluidized beds. Journal of Fluid Mechanics, 2013, 732, 245-281.	1.4	1
154	Sol–Gelâ€Derived, Calciumâ€Based, Copperâ€Functionalised CO ₂ Sorbents for an Integrated Chemical Looping Combustion–Calcium Looping CO ₂ Capture Process. ChemPlusChem, 2013, 78, 92-100.	1.3	33
155	Synthesis of calcium-based, Al2O3-stabilized sorbents for CO2 capture using a co-precipitation technique. International Journal of Greenhouse Gas Control, 2013, 15, 48-54.	2.3	63
156	High-Purity Hydrogen via the Sorption-Enhanced Steam Methane Reforming Reaction over a Synthetic CaO-Based Sorbent and a Ni Catalyst. Environmental Science & Technology, 2013, 47, 6007-6014.	4.6	119
157	Review of Oxygen Carriers for Chemical Looping with Oxygen Uncoupling (CLOU): Thermodynamics, Material Development, and Synthesis. Energy Technology, 2013, 1, 633-647.	1.8	167
158	CaOâ€Based CO ₂ Sorbents: From Fundamentals to the Development of New, Highly Effective Materials. ChemSusChem, 2013, 6, 1130-1148.	3.6	287
159	Sorbentâ€Enhanced Steam Methane Reforming Reaction Studied over a Caâ€Based CO ₂ Sorbent and Ni Catalyst. Chemical Engineering and Technology, 2013, 36, 1496-1502.	0.9	18
160	Magnetic resonance imaging (MRI) study of jet height hysteresis in packed beds. , 2013, , .		0
161	The formation of polygon-shaped patterns in vibrated, cylindrical granular beds. , 2013, , .		0
162	Is axial dispersion within rotating cylinders governed by the Froude number?. Physical Review E, 2012, 86, 061314.	0.8	7

#	Article	IF	CITATIONS
163	Sorbent-Enhanced Methane Reforming over a Ni–Ca-Based, Bifunctional Catalyst Sorbent. ACS Catalysis, 2012, 2, 1635-1646.	5.5	112
164	Influence of the Calcination and Carbonation Conditions on the CO ₂ Uptake of Synthetic Ca-Based CO ₂ Sorbents. Environmental Science & Technology, 2012, 46, 10849-10856.	4.6	91
165	Development of calcium-based, copper-functionalised CO2 sorbents to integrate chemical looping combustion into calcium looping. Energy and Environmental Science, 2012, 5, 6061.	15.6	77
166	Synthesis of Cu-Rich, Al ₂ O ₃ -Stabilized Oxygen Carriers Using a Coprecipitation Technique: Redox and Carbon Formation Characteristics. Environmental Science & Technology, 2012, 46, 3561-3566.	4.6	45
167	Highly Efficient CO ₂ Sorbents: Development of Synthetic, Calcium-Rich Dolomites. Environmental Science & Technology, 2012, 46, 559-565.	4.6	104
168	Validation of a lattice Boltzmann model for gas–solid reactions with experiments. Journal of Computational Physics, 2012, 231, 5334-5350.	1.9	22
169	Critical assessment of two approaches for evaluating contacts between super-quadric shaped particles in DEM simulations. Chemical Engineering Science, 2012, 78, 226-235.	1.9	102
170	On the occurrence of polygon-shaped patterns in vibrated cylindrical granular beds. European Physical Journal E, 2012, 35, 90.	0.7	5
171	Synthesis of Highly Efficient, Caâ€Based, Al ₂ O ₃ ‣tabilized, Carbon Gelâ€Templated CO ₂ Sorbents. Advanced Materials, 2012, 24, 3059-3064.	11.1	199
172	Application of the Sol–Gel Technique to Develop Synthetic Calciumâ€Based Sorbents with Excellent Carbon Dioxide Capture Characteristics. ChemSusChem, 2012, 5, 411-418.	3.6	70
173	Coprecipitated, Copperâ€Based, Aluminaâ€6tabilized Materials for Carbon Dioxide Capture by Chemical Looping Combustion. ChemSusChem, 2012, 5, 1610-1618.	3.6	25
174	Axial transport within bidisperse granular media in horizontal rotating cylinders. Physical Review E, 2011, 84, 041301.	0.8	15
175	Multi-scale magnetic resonance measurements and validation of Discrete Element Model simulations. Particuology, 2011, 9, 330-341.	2.0	10
176	Effect of periodic boundary conditions on granular motion in horizontal rotating cylinders modelled using the DEM. Granular Matter, 2011, 13, 75-78.	1.1	14
177	Comparison of bubble eruption models with two-fluid simulations in a 2D gas-fluidized bed. Chemical Engineering Journal, 2011, 171, 328-339.	6.6	18
178	The production of separate streams of pure hydrogen and carbon dioxide from coal via an iron-oxide redox cycle. Chemical Engineering Journal, 2011, 166, 1052-1060.	6.6	38
179	Tangential velocity profiles of granular material within horizontal rotating cylinders modelled using the DEM. Granular Matter, 2010, 12, 587-595.	1.1	23
180	The kinetics of the reduction of iron oxide by carbon monoxide mixed with carbon dioxide. AICHE Journal, 2010, 56, 1016-1029.	1.8	16

#	Article	IF	CITATIONS
181	In situ gasification and CO2 separation using chemical looping with a Cu-based oxygen carrier: Performance with bituminous coals. Fuel, 2010, 89, 2353-2364.	3.4	76
182	Magnetic resonance studies of a gas–solids fluidised bed: Jet–jet and jet–wall interactions. Particuology, 2010, 8, 617-622.	2.0	20
183	Development of Iron Oxide Carriers for Chemical Looping Combustion Using Solâ^'Gel. Industrial & Engineering Chemistry Research, 2010, 49, 5383-5391.	1.8	82
184	Capture of CO ₂ Using Sorbents of Calcium Magnesium Acetate (CMA). Energy & Fuels, 2010, 24, 3687-3697.	2.5	44
185	Magnetic resonance measurements of high-velocity particle motion in a three-dimensional gas-solid spouted bed. Physical Review E, 2010, 82, 050302.	0.8	11
186	Magnetic Resonance Studies of Fluidization Regimes. Industrial & Engineering Chemistry Research, 2010, 49, 5891-5899.	1.8	22
187	Stabilizing Iron Oxide Used in Cycles of Reduction and Oxidation for Hydrogen Production. Energy & Fuels, 2010, 24, 4025-4033.	2.5	75
188	Laser diagnostic investigation of the bubble eruption patterns in the freeboard of fluidized beds: Simultaneous acetone PLIF and stereoscopic PIV measurements. AICHE Journal, 2009, 55, 1369-1382.	1.8	13
189	Geometrical and hydrodynamical study of gas jets in packed and fluidized beds using magnetic resonance. Canadian Journal of Chemical Engineering, 2009, 87, 517-525.	0.9	27
190	Validation of a discrete element model using magnetic resonance measurements. Particuology, 2009, 7, 297-306.	2.0	105
191	Clean hydrogen production and electricity from coal via chemical looping: Identifying a suitable operating regime. International Journal of Hydrogen Energy, 2009, 34, 1-12.	3.8	223
192	Comparison of ECVT and MR Measurements of Voidage in a Gas-Fluidized Bed. Industrial & Engineering Chemistry Research, 2009, 48, 172-181.	1.8	43
193	Performance of a Novel Synthetic Ca-Based Solid Sorbent Suitable for Desulfurizing Flue Gases in a Fluidized Bed. Industrial & Engineering Chemistry Research, 2009, 48, 7016-7024.	1.8	18
194	Investigation of the Enhanced Water Gas Shift Reaction Using Natural and Synthetic Sorbents for the Capture of CO ₂ . Industrial & Engineering Chemistry Research, 2009, 48, 10284-10291.	1.8	56
195	Different Methods of Manufacturing Fe-Based Oxygen Carrier Particles for Reforming Via Chemical Looping, and Their Effect on Performance. , 2009, , 505-511.		4
196	Experimental Investigation of Two Modified Chemicallooping Compustion Cycles Using Syngas from Cylindersand the Gasification of Solid Fuels. , 2009, , 590-595.		1
197	The Performance of a Novel Synthetic Ca-Based Solid Sorbent Suitable for the Removal of CO2 and SO2 from Flue Gases in a Fluidised Bed. , 2009, , 972-978.		0
198	Synthetic Caâ€based solid sorbents suitable for capturing CO ₂ in a fluidized bed. Canadian Journal of Chemical Engineering, 2008, 86, 356-366.	0.9	114

#	Article	IF	CITATIONS
199	How does the concentration of CO ₂ affect its uptake by a synthetic Caâ€based solid sorbent?. AICHE Journal, 2008, 54, 3308-3311.	1.8	38
200	Spatially resolved measurement of anisotropic granular temperature in gas-fluidized beds. Powder Technology, 2008, 182, 171-181.	2.1	70
201	Magnetic Resonance Imaging of fluidized beds. Powder Technology, 2008, 183, 53-62.	2.1	79
202	Granular temperature: Comparison of Magnetic Resonance measurements with Discrete Element Model simulations. Powder Technology, 2008, 184, 241-253.	2.1	166
203	Magnetic resonance imaging of fluidized beds: Recent advances. Theoretical Foundations of Chemical Engineering, 2008, 42, 469-478.	0.2	13
204	Laser Diagnostic Investigation of the Bubble Eruption Patterns in the Freeboard of Fluidized Beds. 1. Optimization of Acetone Planar Laser Induced Fluorescence Measurements. Industrial & Engineering Chemistry Research, 2008, 47, 5686-5697.	1.8	8
205	Production of Very Pure Hydrogen with Simultaneous Capture of Carbon Dioxide using the Redox Reactions of Iron Oxides in Packed Beds. Industrial & Engineering Chemistry Research, 2008, 47, 7623-7630.	1.8	142
206	Rapid two-dimensional imaging of bubbles and slugs in a three-dimensional, gas-solid, two-phase flow system using ultrafast magnetic resonance. Physical Review E, 2007, 75, 020302.	0.8	40
207	A Study of the Motion and Eruption of a Bubble at the Surface of a Two-Dimensional Fluidized Bed Using Particle Image Velocimetry (PIV). Industrial & Engineering Chemistry Research, 2007, 46, 1642-1652.	1.8	63
208	Rise velocities of bubbles and slugs in gas-fluidised beds: Ultra-fast magnetic resonance imaging. Chemical Engineering Science, 2007, 62, 82-93.	1.9	32
209	Oscillations in gas-fluidized beds: Ultra-fast magnetic resonance imaging and pressure sensor measurements. Powder Technology, 2007, 177, 87-98.	2.1	35
210	Time-of-flight variant to image mixing of granular media in a 3D fluidized bed. Journal of Magnetic Resonance, 2007, 187, 199-204.	1.2	9
211	The nature of the flow just above the perforated plate distributor of a gas-fluidised bed, as imaged using magnetic resonance. Chemical Engineering Science, 2006, 61, 6002-6015.	1.9	72
212	Real-Time Measurement of Bubbling Phenomena in a Three-Dimensional Gas-Fluidized Bed Using Ultrafast Magnetic Resonance Imaging. Physical Review Letters, 2006, 96, 154504.	2.9	74
213	A study of the mixing of solids in gas-fluidized beds, using ultra-fast MRI. Chemical Engineering Science, 2005, 60, 2085-2088.	1.9	38